Biol Cybern (2016) 110:73–80
DOI 10.1007/s00422-016-0680-z

ORIGINAL ARTICLE

Biological Cybernetics

Equivalent linear damping characterization in linear and nonlinear force–stiffness muscle models

Marzieh Ovesy[1] · **Mohammad Ali Nazari**[1] · **Mohammad Mahdavian**[1]

Received: 1 October 2015 / Accepted: 16 January 2016 / Published online: 2 February 2016

Abstract In the current research, the muscle equivalent linear damping coefficient which is introduced as the force–velocity relation in a muscle model and the corresponding time constant are investigated. In order to reach this goal, a 1D skeletal muscle model was used. Two characterizations of this model using a linear force–stiffness relationship (Hill-type model) and a nonlinear one have been implemented. The OpenSim platform was used for verification of the model. The isometric activation has been used for the simulation. The equivalent linear damping and the time constant of each model were extracted by using the results obtained from the simulation. The results provide a better insight into the characteristics of each model. It is found that the nonlinear models had a response rate closer to the reality compared to the Hill-type models.

Keywords Muscle modeling · Hill-type models · Linear damping · Time constant

1 Introduction

Many muscle models have been proposed in order to give a better insight into the muscle behavior toward activations coming from the central nervous system. The most known model in achieving this goal is the Hill's model (Hill 1938). The phenomenological modeling approach based on Hill's model dominates in musculoskeletal systems modeling for simplicity and low computational cost (Siebert et al. 2008).

✉ Marzieh Ovesy
marzieh.ovesy@gmail.com

[1] Mechanical Engineering Department, Faculty of Engineering, University of Tehran, Tehran, Iran

On the basis of Hill's muscle model, several Hill-type models have been emerged. These models consist mainly of three elements: contractile element (CE), series elastic element (SE), and parallel elastic element (PE) in diverse configurations (Zajac 1988; van Soest and Bobbert 1993; Günther and Ruder 2003; Siebert et al. 2008; Haeufle et al. 2012; Winters et al. 2012). The contraction dynamics of muscle has been recorded and described in numerous muscle experiments. CE describes the force–length and the force–velocity dependency of muscle fibers phenomenologically. The muscle fiber velocity depends on the CE force in a hyperbolic relation mostly known as the Hill's relation (Zajac 1988). In a real muscle, the elasticity of CE and the surrounding passive tissues can be represented as elastic elements. These passive structures are usually divided into components thought to act purely in series (SE) and purely in parallel (PE) to the contractile element (CE) in classical Hill-type models. Therefore, two principal Hill-type models have emerged: one in which the parallel elastic element (PE) is arranged in parallel with the CE and the SE; the other, in which the PE is only in parallel with CE (Fig. 1). Both models have been used in the past to represent muscle contraction (Ettema and Meijer 2000; Haenen et al. 2003; Siebert et al. 2008). One of the deficiencies of these models is the lack of inclusion of mass and inertia of the muscle. The output is a one-dimensional force, which is applied to the models between the origin and the insertion points, or sometimes as moments by means of (constant) lever arms (Haeufle et al. 2014). The models inputs are neural muscle stimulation which acts as a force-generating term in CE, and the resulting force modulates through PE and SE.

The study of motor control gives a better insight into the effects the central nervous system has on the functional, goal-directed movement (Cheng et al. 2000). In the mid-sixties, a unique approach for development of a theory for

human motor control was proposed by Asatryan and Feldman (1965a). As a result of a number of experiments, a model called the *A* model emerged. This model was based on the equilibrium point (EP) hypothesis that suggests the active movements to be a result of shifts in the equilibrium state of the motor system. In the mentioned model, the shifts are associated with setting the threshold (*A*) of the stretch reflex in its formulation (Asatryan and Feldman 1965a,b; Feldman 1996). Later this theory was extended and refurbished with more details (Feldman 1974a,b, 1976, 1986). Foisy and Feldman (2006) tested the two major theories of motor control (internal models and threshold control). The first model behaves as position-dependent EMG control which explains that the system counteracts the opposing forces by increasing the muscle activity in proportion to the distance from the initial posture. In contrast, the second model theory fully excludes these opposing forces by shifting thresholds as muscle activation parameter and thus resetting the equilibrium positions to a new posture. In general, two types of functional motor or muscle models provided in the literature by Hill and Feldman could be considered as models with nonlinear springs. The Hill's model is characterized as models with adjustable stiffness due to excluding the reflex effect. On the other hand, including the reflex effect would result in adjustable starting length models that Feldman's model could be considered one of them (Feldman 1966; Shadmehr and Arbib 1992). It was later investigated by Shadmehr and Arbib (1992) that while taking into account the muscle reflex effects, the same level of joint stiffness can be produced by much smaller muscle forces because of the nonlinear stiffness–force relationship.

Mörl et al. (2012) investigated the extent that Hill-type muscle models are able to explain the electromechanical delay (EMD). The EMD is the lag between the changes in the simulation and the force produced in the muscle. In addition, Millard et al. (2013) compared the computational speed and biological accuracy of three musculotendon models: two with an elastic tendon (an equilibrium model and a damped equilibrium model) and one with a rigid tendon. Stearne et al. (2012) also used the muscles force–length–velocity relationship driven from an individually scaled musculoskeletal OpenSim's model in determination of the triceps surae muscles to Achilles tendon force using a Hill-type model. The nonlinear force–velocity also plays a significant role in stabilizing a muscle model and results in lower energy cost. This effect was investigated on computational model of an anguilliform swimmer by Hamlet et al. (2015).

The purpose of this study is to simulate the Hill's and Feldman's muscle models, estimating the equivalent damping and time constant of each, and comparing the results with those obtained by the known models of OpenSim simulation pack. First, Hill's and Feldman's models and their properties for the cat soleus muscle are described. Afterward, the Hill's model isometric contraction with linear passive properties is simulated. Then the equivalent damping and the time constant of each model is evaluated. Analysis of these results allows us to reach a better understanding of the speed, accuracy and stabilization of each muscle model. Due to nonlinear passive properties of muscles, the procedure explained above is once again implemented considering nonlinear passive properties, and the results are compared. We also simulate Hill's muscle using the models in OpenSim. This gives a better insight into their responses.

2 Methods

2.1 Adjustable stiffness model (Hill-type model)

The classical Hill-type model has usually two representations called the [CE + PE] model and [CE + SE] model as illustrated in Fig. 1. The former consists of a contractile component in parallel to an elastic component named as PE and an elastic component in series with the whole model named as SE, whereas in the latter the SE component is in series with the CE part and the combination of these two would be in parallel to the PE component. When modeling solely the active properties of the muscles, there would be no significant difference in these two models; however, the difference would rise when the passive properties of the muscle would come into action.

Siebert et al. (2008) investigated that which representations of Hill's model best describe the muscle response. Comparing the force–velocity relationship, the stiffness and the muscle's yield strains, they concluded that the [CE + PE] model better captures the muscle dynamics. As a result, in order to simulate the muscle contraction, [CE + PE] model was chosen. The force generated in contractile element is a function of the level of activation known as a signal coming from the nervous system to simulate the muscle (F_A), the maximum active isometric force (F_{max}), the force–length (F_L) and the force–velocity characteristics (F_v):

$$F_{CE} = F_L F_v F_A F_{max} \tag{1}$$

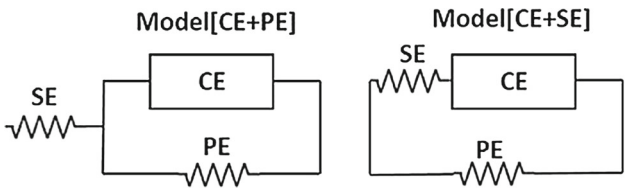

Fig. 1 Hill-type model representations, where (*left*) is the [CE + SE] model and (*right*) is the [CE] model, and both models consist of a series element (SE), a contractile element (CE) and a parallel element (PE)

The level of activation F_A was chosen to be modeled as a ramp starting from 0 at time 0 and reaching the maximum level of activation (1) in 0.1 s (t_{max}) and maintaining this value for the remaining time of the simulation (0.9 s). The activation applied to the muscle is:

$$F_A = \begin{cases} \frac{t}{t_{max}} & \text{if } t < t_{max} \\ 1 & \text{if } t \geq t_{max} \end{cases} \quad (2)$$

The force–velocity relationship, which is illustrated in Fig. 2, is the hyperbola proposed by Hill (1938). The hyperbola is an evident of the damping characteristic of the muscle for concentric contractions explaining that the faster the muscle contracts, the less the force generated (Van Leeuwen and Kier 1997).

$$F_v = \frac{v_{CEmax} - v_{CE}}{v_{CEmax} + (v_{CE}.curv)} \quad \text{if } v_{CEmax} < 0 \quad (3)$$

where $v_{CEmax} < 0$ is the maximal CE shortening velocity and *curve* is a curvature parameter (Siebert et al. 2008).

In an eccentric contraction, the applied force value would grow when the velocity of lengthening increases. Behavior in extension follows another curve rather than the Hill's hyperbola (Katz 1939).

$$F_v = p - (p-1)\frac{v_{CEmax} + v}{v_{CEmax} - curv.k_{ec}.v} \quad \text{if } v_{CEmax} \geq 0 \quad (4)$$

where k_{ec} is an eccentric muscle constant, which can be computed from the difference between the slopes of the force velocity curves on both sides of the zero velocity. If the slope in eccentric section is n times the slope in concentric section, k_{ec} becomes (Nazari 2011):

$$k_{ec} = \frac{n\left(\frac{1}{curv} + 1\right)}{p-1} - \frac{1}{curv} \quad (5)$$

The p parameter, indicating the threshold of the muscle to withstand the elongation, value is 1.8 times of the maximum isometric force. As the muscle contraction is simulated, the eccentric part of the force–velocity function (positive velocities) was ignored.

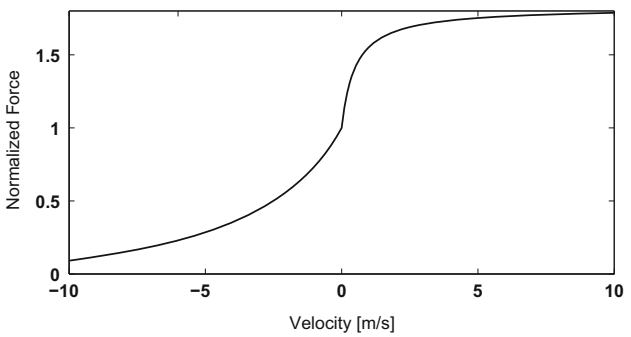

Fig. 2 Hill-type force–velocity curve; negative velocity shows the concentric motion and positive velocity shows the eccentric motion

The CE force–length relation was assumed to be linear as shown in Fig. 3:

$$F_l = \begin{cases} 0 & \text{if } l_{CE} \leq l_4 \\ \frac{f_c}{(l_3 - l_4)}(l_{CE} - l_4) & \text{if } l_4 \leq l_{CE} \leq l_3 \\ \frac{(f_c - 1)}{l_3}(l_{CE} - l_3) + 1 & \text{if } l_3 \leq l_{CE} \leq 0 \\ 1 & \text{if } 0 \leq l_{CE} \leq l_2 \\ \frac{(l_{CE} - l_2)}{(l_2 - l_1)} + 1 & \text{if } l_2 \leq l_{CE} \leq l_1 \\ 0 & \text{if } l_1 \leq l_{CE} \end{cases} \quad (6)$$

where l_{CE} is equal to $l - l_{opt}$, f_c is the force at which the ascending limb changes slope and l_1, l_2, l_3 and l_4 are crucial lengths that the force–length relation slope changes (Siebert et al. 2008).

Winters et al. (2012) proposed the $F_{SE}(\triangle l_{SE})$ relationship as:

$$F_{SE}(\triangle l_{SE}) = \begin{cases} \frac{F_1}{(e^{k_{sh}} - 1)} \cdot \left(e^{\frac{(k_{sh}.\triangle l_{SE})}{(\triangle l_{SE1})}} - 1\right) & \text{if } 0 < \triangle l_{SE} < \triangle l_{SE1} \\ F_1 + k.(\triangle l_{SE} - \triangle l_{SE1}) & \text{if } \triangle l_{SE1} < \triangle l_{SE1} \end{cases} \quad (7)$$

where $\triangle l_{SE1}$ and F_1 are the elongation and the force at which the force–elongation relation changes from exponential to linear, respectively. k was calculated from $\triangle l_{SEC1}$, F_1, the dimensionless shape parameter k_{sh} and the constraint of equal stiffness at the place where $\triangle l_{SEC}$ equals $\triangle l_{SEC1}$ (Siebert et al. 2008). In model [CE + PE], the PE influences the intrinsic contraction dynamics. A PE force–elongation relationship represented as $F_{PE}(\triangle l_{PE})$ depending on k_1 and k_2 was taken from (Brown et al. 1996)

$$F_{PE}(\triangle l_{PE}) = k_1.(e^{k_2.\triangle l_{PE}} - 1) \text{ if } \triangle l_{PE} > 0 \quad (8)$$

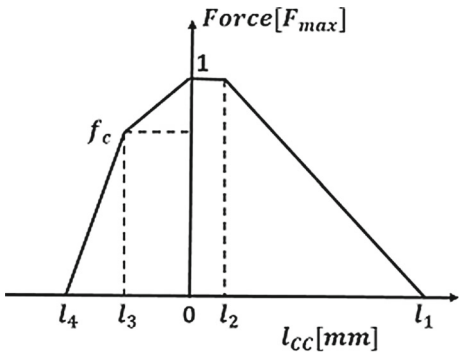

Fig. 3 The force–length relationship was normalized relative to F_{max} and considered as a linear model . l_4 and l_1 determining the width of the force–length relationship. l_3 is the length at which the ascending limb changes slope, f_c is the corresponding normalized force, and l_2 is equal to the width of the plateau

Table 1 Single muscle parameters of model [CE + PE] based on the corresponding ramp experiments (Siebert et al. 2008)

Model [CE]	
Solution 1	
$f_c[F_{max}]$	0.51
l_1 [mm]	8
l_2 [mm]	4
l_3 [mm]	−14
l_4 [mm]	−24
curve	9.5
F_1 [N]	8.9
k_1 [N]	0.0064
k_2 [(mm)$^{-1}$]	0.414
$k\left[\frac{N}{mm}\right]$	8.2
F_{max}[N]	20.5
k_{sh}	2.5
$v_{CEmax}\left[\frac{mm}{s}\right]$	−152
$l_{opt.exp}$[mm]	53
p	1.8

Two characterizations of the passive elements have been implemented. First they are linearized at starting position (linear model) and then the nonlinear characteristics are considered (nonlinear model). In the linear model, the slope at the starting position is considered as linear stiffness of passive elements. For SE the stiffness becomes:

$$k_{SE} = \begin{cases} \frac{F_1.k_{sh}}{(e^{k_{sh}}-1).\triangle l_{SE1}} & \text{if } 0 < \triangle l_{SE} < \triangle l_{SE1} \\ k & \text{if } \triangle l_{SE1} \leq \triangle l_{SE} \end{cases} \quad (9)$$

The passive properties of the muscle and the Hill's activation parameters are shown in Table 1.

2.2 Adjustable starting length model (Feldman's model)

The Feldman and Hill-type muscle models have the similar passive properties. Their difference emerges in the contractile element function (active properties).

Feldman (1986) proposed a model considering the force generated in contractile component as a nonlinear function of activation level and the velocity:

$$F_{CE} = f(L, v, l_{threshold}) \quad (10)$$

In Feldman's model, the activation level depends on the difference between the muscle length and the zero-force length ($l_{thereshold}$), which is the control parameter (Feldman 1986). This model is considered as an adjustable starting length mode, where muscle stiffness changes as a nonlinear function of force for different activation levels. Feldman (2011) described that for a given activation command, muscle contractile force depends on combination of the stretch–reflex mechanism and the force–length characteristic, which is an exponential curve called the invariant characteristics (IC):

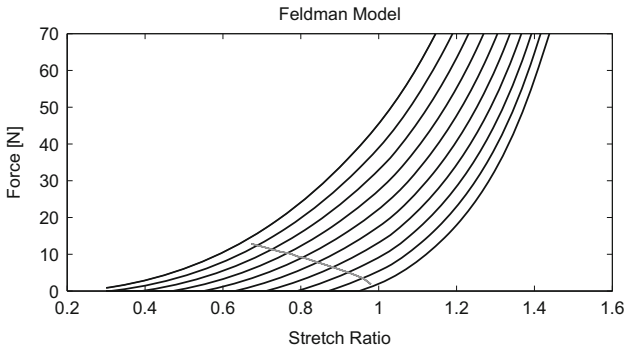

Fig. 4 Feldman muscle invariant characteristics (IC) at a given velocity (Nazari et al. 2013)

$$F_{CE-Feldman} = F_{max} \times \left(\exp\frac{[l(t-d_e) - l_{threshold} + \mu(v(t-d_e))]^+}{l_c} - 1\right) \quad (11)$$

where F_{max} is the maximum force generation capacity of a muscle and is a function of the physical cross-sectional area of it, $l_{threshold}$ is zero-force length (threshold length), l_c is the characteristic length, v is muscle velocity and μ is a damping coefficient. Both muscle length and velocity in this equation are delayed values at time $t - d_e$. $[]^+$ means that the force is equal to zero if the expression within $[]^+$ is negative.

Pilon and Feldman (2006) have also proposed a threshold model for the torque applied to human elbow as an exponential function of the adjustable length as below:

$$M = a\left(\exp\left(\frac{A}{l_c}\right) - 1\right) \quad (12)$$

where a acts as the maximum moment that the joint is able to insert and A is considered as:

$$A = \frac{1}{1+r}(l(t-d_e) - l_{threshold} + \mu v(t-d_e)) \quad (13)$$

where d_e, μ and $l_{threshold}$ have the similar definitions as our representation of Feldman's model and r is a weight coefficient with a value of 0.05. The effect of r in this research can be simulated by replacing l_c with $l_c(1+r)$. As a result, the two models are simillar exept for this difference.

A passive force should be added to this active force to take into account the passive mechanical property of the muscle (Nazari et al. 2013). Muscle invariant characteristics (IC) at a given velocity is shown in Fig. 4, where the gray path shows an example of a voluntary contraction of muscle when motor commands (starting lengths) are changing.

3 Results

The simulation was performed under the assumption of isometric contraction. In modeling the linear passive properties, linear springs were used, and while simulating the nonlinear model, the nonlinear passive functions replaced the linear springs.

The muscle damping property is defined through its force–velocity characteristic. In order to evaluate the damping characteristic of Hill's model, the force–velocity function was removed and replaced by a linear damper with the coefficient of B.

The Feldman's $l_{\text{threshold}}$ was chosen to be a ramp function starting from $l_{\text{th}-\text{initial}}$ that was chosen to be equal to l_{opt} (the optimum muscle length), reaching $l_{\text{th}-\text{final}}$ in 0.1 s. The value of $l_{\text{th}-\text{final}}$ was chosen in such a manner to provide the same maximum force reached by Hill's model at the same muscle length.

In the literature the characteristic length l_{c} varies between 9 mm (Laboissiere et al. 1996) and 25 mm (Buchaillard et al. 2006) with a role that is to stabilize the model. The value of 8.93 mm was chosen for l_{c} which is close to the range mentioned above and obtained by Asatryan and Feldman (1965b) from torque–angle curves for the human elbow (Laboissiere et al. 1996).

The parameter μ is called the damping coefficient. In the physiological literature, damping is associated with regulation of muscle force as a function of velocity. In contrast, the damping coefficient, μ, characterizes the dependence of muscle's threshold length on velocity. Both proprioceptive feedback and muscle intrinsic properties are velocity dependent and thus contribute to the force-related damping in a nonlinear way. The component of force-related damping dependent on proprioceptive feedback is, to a first approximation, proportional to the product of muscle stiffness and the coefficient μ (St-Onge et al. 1993). Thus, even though μ is considered, for simplicity, the same for all muscles and constant for a given movement (0.05 s), the force-related damping may still vary as a function of stiffness both for a single muscle and between muscles (Laboissiere et al. 1996).

Considering the fact that the Hill's force–length curve uses the difference between current muscle length and optimal length as its characteristic length, the Feldman's model uses the current muscle length. Having the current muscle length, the following relation can be used to compute the threshold length:

$$l_{\text{threshold}} = l - l_c \ln\left(\frac{F_{\text{in}}}{F_{\max}} + 1\right) \tag{14}$$

where F_{in} and l are the current force and length of the muscle and l_{c} and $F_{\max}$ have the values defined earlier in the text.

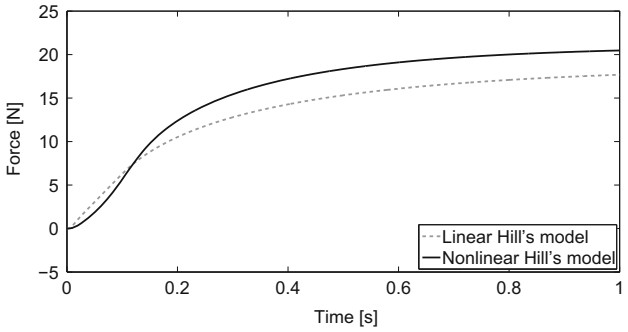

Fig. 5 Hill's muscle model force–time plot considering linear passive properties (*black line*) and nonlinear passive properties (*gray dashed line*)

In this section we present a simulation of the model described above. The simulation was run using ode45 solver that has a variable time step in order to achieve the tolerance specified. The tolerance was set to 0.001 ms. The assumption of linear passive elements was made followed by the implementation of nonlinear passive elements. As can be seen in Fig. 5, the maximum force generated taking into account nonlinearity is 20.47 N which is greater than the force with linear assumption 17.68 N.

In addition, there exists a little offset between the force obtained during nonlinear simulation and $F_{\max}$. This offset could be due to the errors existing in consideration of the mean value of several experiments. The Hill's model with nonlinear passive properties was also implemented in the OpenSim software (Delp et al. 2007). OpenSim is considered as a software that provides its users with the ability to observe and analyze the forces generated during movement in different muscles of the body.

In order to simulate the Hill's response in OpenSim, the same activation as in Hill's model (Eq. 2) is applied on a model of an isometric muscle. The muscle modeling used for this purpose is based on the modeling proposed by Millard et al. (2013).

The force applied to the muscle in the Millard's model is:

$$f^M = f_o^M\left(\alpha, f^L(\hat{l}^M), f^V(\hat{v}^M)\right) + f^{\text{PE}}(\hat{l}^M) \tag{15}$$

where the first term (f_o^M) is the Hill's active force that is a function of α (activation), f_L (active force–length relationship), f_v (active force–velocity relationship), and the second term (f^{PE}) is the passive force which is a function of the current muscle length ($\hat{l}^M$). Changing the active force–length, active force–velocity, the maximum isometric force, and the optimal muscle length to be the same as the Hill's model, the plots shown in Fig. 6 are obtained.

As it can be seen Fig. 6, both models have reached their desired maximum isometric force; however, there exists a small difference between the results in the transient part. This

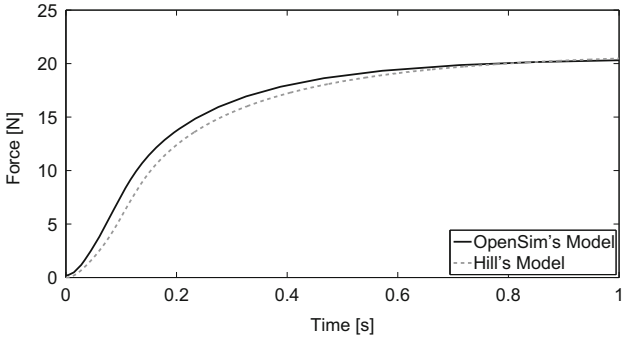

Fig. 6 The Hill's model (*gray line*) and the OpenSim's model (*black line*)

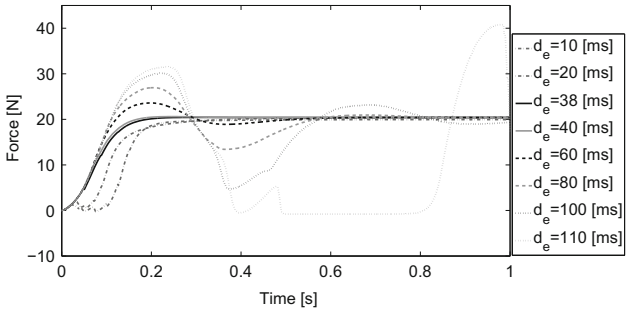

Fig. 7 The effect of reflex delay on the stability of Feldman's muscle model + Hill's force–velocity term

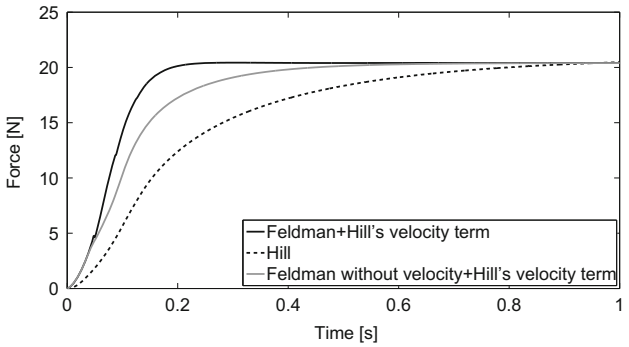

Fig. 8 Hill's muscle model force–time plot (*black dashed line*), Feldman's muscle model combined with Hill's force–velocity term (*black line*) and Feldman's muscle model without its velocity term combined with Hill's force–velocity term (*gray line*)

could be due to the different passive and active properties considered for each modeling. As for the active force–length relation, the OpenSim ignores the 0 to l_2 part in Fig. 3 where the normalized force has the constant value of one. The more these two obey the same formulation, the more similar the results would become.

Using Eq. 14 and the maximum force of 20.47 N achieved at active length of 44.3 mm, the $l_{\text{th}-\text{final}}$ was set to 38.11 mm. Therefore, the l_{th} starts from 53 mm (l_{opt}) to 44.3 mm, $l_{\text{th}-\text{final}}$ during the first 0.1 ms.

In the literature, different values of the reflex delay have been reported. For example, Luschei and Goldberg (2011) used 10 ms delay for mastication in monkeys and Buchaillard et al. (2009) used 17 ms in tongue muscle modeling. Pilon and Feldman (2006) have studied the effect of reflex delay on the stability of the inserted torque to the elbow movements and illustrated that their model is stable from 30 to 100 ms. For this purpose we have studied the effect of changing the delay values on output response. It is shown in Fig. 7 that the proposed model in this study remains stable for reflex delays up to to 100 ms and the response becomes unstable as the reflex delay becomes higher than 100 ms. As it can be seen, the delay values less than 38 ms generates oscillations for the start of activation and the values more than 38 ms generates overshooting in force values at the beginning of response. Hence we picked up the delay value as 38 ms in our simulations.

In order to evaluate the damping characteristic of each model, the Feldman's muscle model was simulated. The resulting oscillations were not damped during the simulation time, which could be an evidence of the model's very low damping characteristic. According to this observation, the Hill's force–velocity term was added to the Feldman's model in order to damp the oscillations. The effect of the Feldman velocity term was also a matter of interest. As a result, two different models including and excluding the Feldman's velocity term were considered in Fig. 8. The results show that there is a little difference between the two proposed models, compared to the difference they have with Hill's model. Therefore, the Feldman's damping characteristic is not significant compared to the Hill's force–velocity term. The damping coefficient (B) introduced via the model's velocity term was calculated by omitting the force–velocity terms and replacing them with a damper that provides the exact maximum force which had been achieved while using those terms. The muscle mass was needed in this part which was assumed to be 3.4 g (Scott et al. 1996). This is the mean value of several experiments conducted on cat's soleus muscle. It can be seen in Fig. 9 that the damping coefficient of Hill's model is 0.98 $\frac{\text{N s}}{\text{mm}}$, whereas the proposed Feldman's combined model with Hill's force–velocity term is 2 $\frac{\text{N s}}{\text{mm}}$ as shown in Fig. 10. In addition, Fig. 11 shows the effect of omitting the Feldman's velocity term on the model mentioned earlier resulting in damping of 1.5 $\frac{\text{N s}}{\text{mm}}$. This is an evidence that the Feldman's model velocity term would enhance the damping ability of the model. On the other hand, it is possible to conclude the fact that combined Feldman's model has a better damping characteristic than the model proposed by Hill.

The time constant was chosen to be the time the muscle force reaches 63.2 % of its final value. It can be seen in Fig. 8 that the time constant of Feldman's combined model

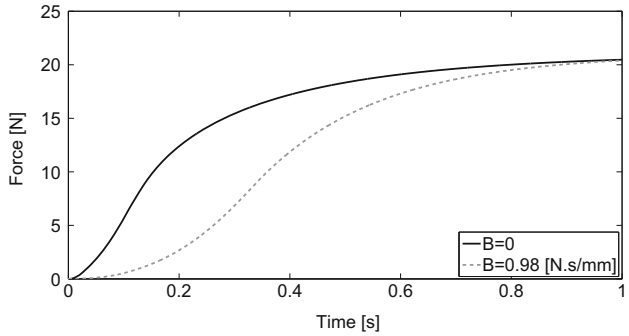

Fig. 9 The equivalent damping characteristic of Hill's muscle model

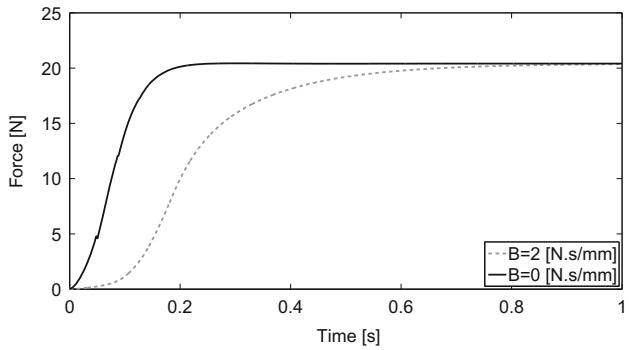

Fig. 10 The equivalent damping characteristic of Feldman's muscle model + Hill's force–velocity term

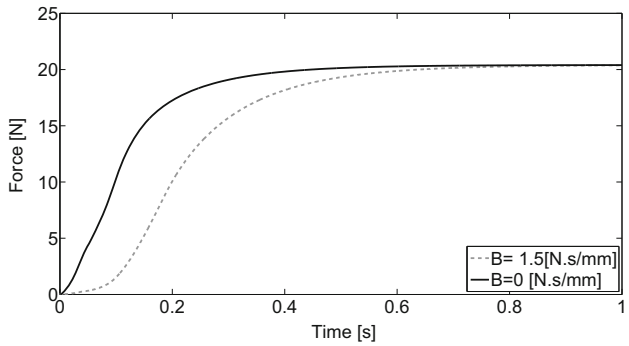

Fig. 11 The equivalent damping characteristic of Feldman's muscle model (excluding its own velocity term) + Hill's force–velocity term

with Hill's force–velocity term was 0.09 s, while excluding the Feldman's velocity term resulted in the time constant of 0.12 s. The time constant of the Hill's model was 0.21 s. This could be an evidence of the fast response of Feldman's model to the activation, and the effect of Feldman's velocity term in enhancing the time constant. The results are shown in Table 2.

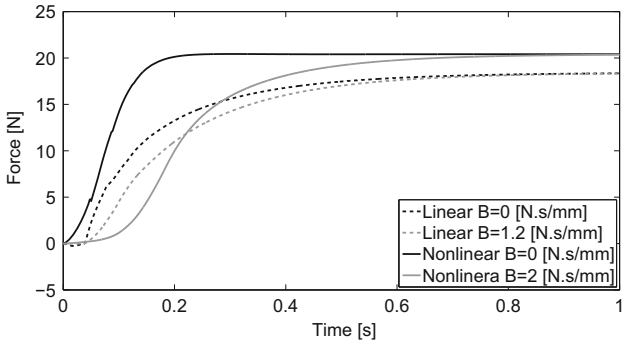

Fig. 12 The effect of nonlinearity on damping and time constant of Feldman's muscle model + Hill's force–velocity term

It is shown in Fig. 12 that the linear passive properties produce less force than the nonlinear ones. As expected, the damping characteristic for the linear Feldman's muscle is 1.2 $\frac{\text{N s}}{\text{mm}}$ which is less than 2 $\frac{\text{N s}}{\text{mm}}$ that is achieved by the nonlinear one. In addition, Fig. 12 implies that nonlinearity would enhance the time constant by 0.03 s, helping the muscle in reaching its desired maximum force in less time.

4 Conclusion

We have simulated Hill's model and proposed a new muscle model combining the Feldman's stretch reflex force with Hill's force-velocity term during isometric contraction. The modeling, numerical analysis and some comparison with the OpenSim software which provides its users with a vast variety of muscle simulations were presented in this article. The equivalent damping characteristic and the time constant for three different models were computed. As far as nonlinear passive properties are considered instead of linear properties, the ability of the model to damp the oscillations and show a closer response to the stimuli coming from the central nervous system would improve. A new model using Feldman's formulation and taking advantage of the Hill's velocity term while taking into account the nonlinear passive properties was proposed. The model has displayed an excellent behavior toward isometric simulation, and has a time constant closer to reality and a higher damping characteristic than other models.

Table 2 Time constant and equivalent damping of three nonlinear models

Models	Damping coefficient $\left[\frac{\text{N s}}{\text{mm}}\right]$	Time constant [s]
Hill	0.98	0.21
Feldman without velocity term + Hill's velocity term	1.5	0.12
Feldman + Hill's velocity term	2	0.09

The present study can be extended in many directions. For example, different activation schemes such as isotonic activation will shed light on other features of the proposed model; modeling the Feldman's muscle model in OpenSim enables a better comparison on a unique platform.

References

Asatryan DG, Feldman AG (1965a) Functional tuning of the nervous system with control of movement or maintenance of a steady posture: I. Mechanographic analysis of the work of the joint or execution of a postural task. Biophysics 10(5):925–934

Asatryan DG, Feldman AG (1965b) Functional tuning of the nervous system with control of movement or maintenance of a steady posture: I. Mechanographic analysis of the work of the joint or execution of a postural task. Biophysics 10(5):925–934

Brown IE, Scott SH, Loeb GE (1996) Mechanics of feline soleus: Ii design and validation of a mathematical model. J Muscle Res Cell Motil 17(2):221–233

Buchaillard S, Perrier P, Payan Y (2006) The study of motor control seeks to determine how the central nervous system effects functional, goal-directed movement. In: Proceedings of the 7th international seminar on speech production, vol 17, pp 403–410

Buchaillard S, Perrier P, Payan Y (2009) A biomechanical model of cardinal vowel production: muscle activations and the impact of gravity on tongue positioning. J Acoust Soc Am 126(4):2033–2051

Cheng EJ, Brown IE, Loeb GE (2000) Virtual muscle: a computational approach to understanding the effects of muscle properties on motor control. J Neurosci Methods 101(2):117–130

Delp SL, Anderson FC, Arnold AS, Loan P, Habib A, John CT, Guendelman E, Thelen DG (2007) OpenSim: open-source software to create and analyze dynamic simulations of movement. Biomed Eng IEEE Trans 54(11):1940–1950

Ettema GJ, Meijer K (2000) Muscle contraction history: modified hill versus an exponential decay model. Biol Cybern 83(6):491–500

Feldman A (1974a) Change in the length of the muscle as a consequence of a shift in equilibrium in the muscle-load system. Biophysics 19:544–548

Feldman A (1974b) Control of the length of the muscle. Biophysics 19(2):766–771

Feldman AG (1966) Functional tuning of nervous system with control of movement or maintenance of a steady posture. 2. Controllable parameters of muscles. Biophys USSR 11(3):565

Feldman AG (1976) Control of postural length and force of a muscle: advantages of the central co-activation of alpha and gamma static motoneurons. J Biophys 19:771–776

Feldman AG (1986) Once more on the equilibrium-point hypothesis (λ model) for motor control. J Mot Behav 18(1):17–54

Feldman AG (1996) Functional tuning of the nervous system with control of movement or maintenance of a steady posture. iii. controllable parameters of the muscle. J Biophys 11:766–775

Feldman AG (2011) Space and time in the context of equilibrium-point theory. Wiley Interdiscip Rev Cognit Sci 2(3):287–304

Foisy M, Feldman AG (2006) Threshold control of arm posture and movement adaptation to load. Exp Brain Res 175(4):726–744

Günther M, Ruder H (2003) Synthesis of two-dimensional human walking: a test of the λ-model. Biol Cybern 89(2):89–106

Haenen WP, Rozendaal LA et al (2003) Stability of bipedal stance: the contribution of cocontraction and spindle feedback. Biol Cybern 88(4):293–301

Haeufle D, Günther M, Bayer A, Schmitt S (2014) Hill-type muscle model with serial damping and eccentric force-velocity relation. J Biomech 47(6):1531–1536

Haeufle D, Günther M, Blickhan R, Schmitt S (2012) Proof of concept: model based bionic muscle with hyperbolic force-velocity relation. Appl Bionics Biomech 9(3):267–274

Hamlet C, Fauci LJ, Tytell ED (2015) The effect of intrinsic muscular nonlinearities on the energetics of locomotion in a computational model of an anguilliform swimmer. J Theor Biol 385:119–129

Hill A (1938) The heat of shortening and the dynamic constants of muscle. Proc R Soc Lond B Biol Sci 126(843):136–195

Katz B (1939) The relation between force and speed in muscular contraction. J Physiol 96(1):45–64

Laboissiere R, Ostry DJ, Feldman AG (1996) The control of multimuscle systems: human jaw and hyoid movements. Biol Cybern 74(4):373–384

Luschei ES, Goldberg LJ (2011) Neural mechanisms of mandibular control: mastication and voluntary biting. In: Comprehensive Physiology. Wiley, pp 1237–1274

Millard M, Uchida T, Seth A, Delp SL (2013) Flexing computational muscle: modeling and simulation of musculotendon dynamics. J Biomech Eng 135(2):021005

Mörl F, Siebert T, Schmitt S, Blickhan R, Guenther M (2012) Electromechanical delay in hill-type muscle models. J Mech Med Biol 12(05):1250085

Nazari MA (2011) Biomechanical face modeling: control of orofacial gestures for speech production. PhD thesis, Université de Grenoble

Nazari MA, Perrier P, Payan Y (2013) A muscle model based on feldman's lambda model: 3d finite element implementation. arXiv preprint arXiv:1307.2809

Pilon J-F, Feldman AG (2006) Threshold control of motor actions prevents destabilizing effects of proprioceptive delays. Exp Brain Res 174(2):229–239

Scott SH, Brown IE, Loeb GE (1996) Mechanics of feline soleus: I. Effect of fascicle length and velocity on force output. J Muscle Res Cell Motil 17(2):207–219

Shadmehr R, Arbib MA (1992) A mathematical analysis of the force-stiffness characteristics of muscles in control of a single joint system. Biol Cybern 66(6):463–477

Siebert T, Rode C, Herzog W, Till O, Blickhan R (2008) Nonlinearities make a difference: comparison of two common hill-type models with real muscle. Biol Cybern 98(2):133–143

St-Onge N, Qi H, Feldman AG (1993) The patterns of control signals underlying elbow joint movements in humans. Neurosci Lett 164(1):171–174

Stearne SM, Rubenson J, Alderson J (2012) Investigation of running foot strike technique on achilles tendon force using ultrasound techniques and a hill-type model. J Foot Ankle Res 5(1):1–2

Van Leeuwen J, Kier WM (1997) Functional design of tentacles in squid: linking sarcomere ultrastructure to gross morphological dynamics. Philos Trans R Soc Lond B Biol Sci 352(1353):551–571

van Soest AJ, Bobbert MF (1993) The contribution of muscle properties in the control of explosive movements. Biol Cybern 69(3):195–204

Winters JM, Woo SL, Delp I (2012) Multiple muscle systems: biomechanics and movement organization. Springer, Berlin

Zajac FE (1988) Muscle and tendon: properties, models, scaling, and application to biomechanics and motor control. Crit Rev Biomed Eng 17(4):359–411